Dryout Phenomena in a Three-Phase Fixed-Bed Reactor

Zhen-Min Cheng, Abdulhakeim M. Anter, Xiang-Chen Fang, Qiong Xiao, and Wei-Kang Yuan
East China University of Science and Technology, Shanghai 200237, P. R. China

Suresh K. Bhatia
Dept. of Chemical Engineering, The University of Queensland, Brisbane, QLD 4072, Australia

Understanding the mechanism of liquid-phase evaporation in a three-phase fixed-bed reactor is of practical importance, because the reaction heat is usually 7–10 times the vaporization heat of the liquid components. Evaporation, especially the liquid dryout, can largely influence the reactor performance and even safety. To predict the vanishing condition of the liquid phase, Raoult's law was applied as a preliminary approach, with the liquid vanishing temperature defined based on a liquid flow rate of zero. While providing correct trends, Raoult's law exhibits some limitation in explaining the temperature profile in the reactor. To comprehensively understand the whole process of liquid evaporation, a set of experiments on inlet temperature, catalyst activity, liquid flow rate, gas flow rate, and operation pressure were carried out. A liquid-region length-predicting equation is suggested based on these experiments and the principle of heat balance.

Introduction

Operation of a three-phase fixed-bed reactor is a challenging task when the liquid phase exhibits substantial volatility. In this case, evaporation of the liquid phase due to the heat of the reaction will complicate both the reaction and transport phenomena in the flow direction. Depending upon the magnitude of the reaction heat, the evaporated fraction of the liquid mixture can change from 0 to 1, and correspondingly, the reactor operation can change from a fully liquid phase to a fully gas phase, and the catalyst filling condition will evolve from a fully wetted to a partially wetted, and ultimately to a completely dry condition.

The effect of evaporation of volatile compounds on reactor performance has been considered important for a variety of systems. Singh and Carr (1983) studied the effect of solvent evaporation on oil production and total coal conversion in the solvent refined coal. Ramakrishna et al. (1985) studied the effect of vaporization of the liquid feed components on reactor performance for hydrogenation of naphthalene dissolved in a diluting solvent. Smith and Satterfield (1986) and LaVopa and Satterfield (1988) studied the effect of vapor–liquid flow ratio and vapor–liquid equilibrium on the performance of a trickle-bed reactor. More recently, a new concept on the basis of continuous phase-transitional operation has been developed for process intensification (Cheng et al., 2001a,b; 2002). The concept has been proved successful for benzene hydrogenation in the production of cyclohexane, and a pilot plant study at a capacity of 5,000 t/a cyclohexane is in progress.

Over the last three decades, studies on evaporation of the liquid phase in multiphase fixed-bed reactors have been confined to two basic aspects. One is the experimental work on reactor performance, as conducted by Sedriks and Kenney (1973), Hanika et al. (1975, 1976, 1977, 1986, 1999), Ruzicka and Hanika (1994), and Castellari et al. (1997). Another is the catalyst-scale study on the physiochemical aspects, as reported by Kim and Kim (1981a,b), Hu and Ho (1987), Bhatia (1988, 1989), Jaguste and Bhatia (1991), Waston and Harold (1993, 1994), as well as Hessari and Bhatia (1996). In spite of these efforts, reactor-scale description of the evaporation of the liquid is still absent, which is most likely related to the difficulty in direct observation and measurement of the liquid due to the opacity of the reactor wall and the catalyst support.

In the present work, the process of liquid evaporation has been systematically evaluated. For this purpose, Raoult's law

---

Correspondence concerning this article should be addressed to Z.-M. Cheng.
Current address of X.-C. Fang: Fushun Petrochemical Research Institute, Fushun 113001, P.R. China.

is applied to provide a theoretical guideline, and specific experiments have been conducted to verify the validity of the theory.

Theoretical Development

In a previous article (Kheshgi et al., 1992), Raoult's law was introduced to account for the variations in the gas and liquid molar flow rates along the reactor, and the liquid flow rate of zero was considered identical to the disappearance of the liquid phase. However, while the validity of the approach is plausible, it was not verified experimentally. In a subsequent article by Khadilkar et al. (1999), a similar approach was followed.

In the present work, as well, we utilize Raoult's law, which has been extensively used in the description of gas–liquid equilibrium in a closed system. However, Raoult's law is extended here to a flowing system accompanied by a reaction, as described by Eq. 1

$$A(\mathrm{l}) + B(\mathrm{g}) \rightarrow C(\mathrm{l}). \tag{1}$$

In the system chosen for the present study, A, B, and C correspond to benzene, hydrogen, and cyclohexane, respectively. The balance equations are established below.

For the vapor phase:

$$y_A + y_B + y_C = 1. \tag{2}$$

For the liquid phase:

$$x_A + x_B + x_C = 1. \tag{3}$$

Equations 1 and 2 are related through the equilibrium relations:

$$y_A = K_A x_A \qquad \text{and} \qquad y_C = K_C x_C. \tag{4}$$

Assuming the conversion of reactant A to be α, the molar flow rates of the components are given as

$$F_A = F_A^0(1-\alpha) \tag{5}$$

$$F_B = (M-\alpha)F_A^0 \tag{6}$$

$$F_C = F_C^0 + \alpha F_A^0, \tag{7}$$

where M is the ratio of feed flow rate of hydrogen to that of benzene, that is, $F_B^0 = MF_A^0$. Equations 5–7 provide the total flow rate:

$$F_l + F_v = (1+M-\alpha)F_A^0 + F_C^0, \tag{8}$$

where F_l is the flow rate of liquid and F_v is that of the vapor. Assuming negligible solubility of hydrogen in the liquid, that is, $x_B \ll 1$, Eqs. 2–4 and the definition of y_B,

$$y_B = \frac{F_B}{F_v} \tag{9}$$

provide the relation

$$F_v = \frac{(M-\alpha)F_A^0}{1-K} \tag{10}$$

for the vapor-phase flow rate. Here the gas–liquid equilibrium constant, K, is used instead of K_A and K_C, since the physical properties of A and C are similar.

The liquid flow rate is now obtained from Eqs. 8 and 10 as:

$$F_l = (1+M-\alpha)F_A^0 + F_C^0 - \frac{(M-\alpha)F_A^0}{1-K}. \tag{11}$$

It should be noted that in benzene hydrogenation, M is always greater than 3, which is the stoichiometric ratio of hydrogen to benzene. Therefore, the parameter α can be neglected in comparison with M, since the conversion of reactant A in the liquid phase is normally less than 0.15, in view of the liquid vaporization heat being one-tenth to one-seventh of the reaction heat. Consequently, Eq. 11 can be reduced to

$$F_l = (1+M)F_A^0 + F_C^0 - \frac{MF_A^0}{1-K}. \tag{12}$$

Since A and C have similar physical properties, $F_A^0 + F_C^0$ can be lumped as the total liquid flow rate F_l^0, and therefore the hydrogen flow rate MF_A^0 can be replaced by NF_l^0, with N being the dimensionless flow rate of hydrogen with respect to F_l^0. Equation 12 is therefore reduced to

$$F_l = (1+N)F_l^0 - \frac{NF_l^0}{1-K}. \tag{13}$$

From Eq. 13 it is seen that liquid flow rate decreases from F_l^0 to F_l in the presence of hydrogen. In addition, by increasing the system temperature, F_l can decrease to zero, since the gas–liquid equilibrium constant K increases with temperature. The vanishing condition of the liquid flow rate is therefore obtained by setting $F_l = 0$ in Eq. 13, which leads to

$$K = \frac{1}{1+N}. \tag{14}$$

Following Raoult's law, the equilibrium constant, K, can be represented as the ratio of the saturation pressure of liquid phase at temperature, T, to the total pressure of the system, that is,

$$K = \frac{P_A^0(T)}{P_{\text{sum}}}, \tag{15}$$

which has been employed by Kheshgi et al. (1992). Combining Eqs. 14 and 15 provides

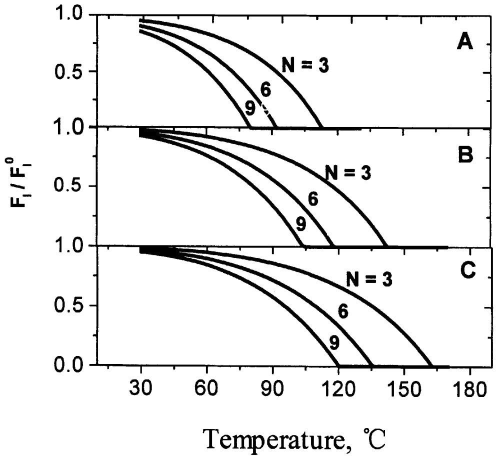

Figure 1. Fraction of liquid not evaporated under different operating conditions.

P_{sum}: A—1.0 MPa; B—2.0 MPa; C—3.0 Mpa.

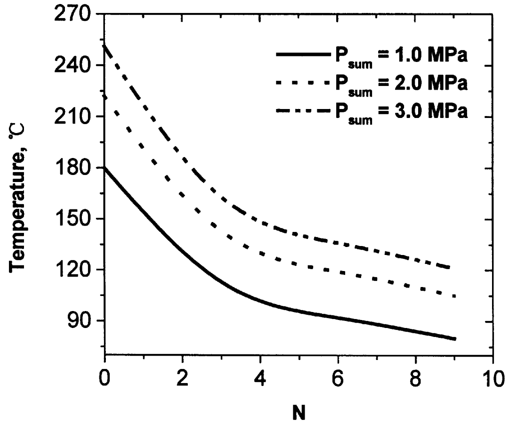

Figure 2. Liquid vanishing temperature under different pressures and gas-to-liquid molar flow-rate ratios.

$$\frac{P_A^0(T_v)}{P_{sum}} = \frac{1}{1+N}, \tag{16}$$

where T_v is the temperature at the point at which liquid vanishes in the reactor. Equation 16 indicates that this temperature is not only dependent on system pressure, but also on the ratio of gas-to-liquid molar flow rate, N. Assuming that the feed gas is composed of pure B, while the liquid feed is a mixture of A and B. The criterion for liquid vanishing is obtained as below:

$$\frac{F_l^0}{F_B^0} = \frac{P_A^0(T_v)}{P_{sum} - P_A^0(T_v)}. \tag{17}$$

Here the saturation vapor pressure P_A^0 has been calculated with the Lee–Kesler equation as given in Reid et al. (1987).

The theoretical results from Eqs. 13 and 17 are plotted in Figures 1 and 2. It is seen in Figure 1 that the amount of liquid not vaporized is a function of the system temperature, the gas-to-liquid flow-rate ratio, as well as the system pressure. Since a zero liquid flow rate means the disappearance of the liquid, the liquid vanishing temperature, T_v, can be obtained from Figure 1 at $F_l = 0$, and the results are given in Figure 2. It shows that the liquid can disappear at a much lower temperature in the presence of hydrogen, which is reasonable thermodynamically.

Experimental Studies

Experiments were carried out in a three-phase fixed-bed reactor with gas and liquid flowing concurrently upward. The reactor was heated by electricity and kept adiabatic with glass-wool insulation. Temperature profiles along the reactor length were measured by means of 12 thermocouples inserted through the reactor wall. Two kinds of catalysts—Catalyst A with 0.5% Pd supported over Al_2O_3, and Catalyst B with Ni–B amorphous alloy supported over Al_2O_3—were employed. Independent experiments demonstrated that Catalyst A was less active, with an activity about one-third of Catalyst B. A detailed description for the flow diagram is available elsewhere (Cheng et al., 2001a).

Results and Discussion

Experimental evaluation of the liquid phase

Vaporization of the liquid phase can lead to depletion of the liquid phase and consequently to partial wetting or even dryout of the reactor. Presumably, the liquid flow rate should be zero once the vanishing temperature is attained, and therefore there will be no liquid region in the reactor once the inlet temperature is above the vanishing temperature. To identify the validity of this assumption, experiments under the inlet temperatures above T_v will provide the most rigorous demonstration.

Reactor performances under five inlet temperatures (130°C, 140°C, 150°C, 160°C, and 170°C) are shown in Figures 3. In these experiments, the vanishing temperature, T_v, is predicted to be 117°C, which is 13°C, 23°C, 33°C, 43°C, and 53°C lower than the respective inlet temperature. It would appear that under all these conditions, the liquid can exist above the predicted vanishing temperature, T_v, which could be deduced from the flat temperature profile at the entry of the reactor. The flat temperature profile in the entry region should be explained as a result of the heat balance between the evaporation of liquid and reaction heat. To clarify the boundary between the liquid- and the gas-phase regions, dashed lines are plotted by connecting the observed phase-transition points. To further verify the validity of the assumption on the corresponding relationship between the flat temperature profile and liquid region, reaction-rate dependence on benzene concentration may be explored.

It is known that under the liquid condition the reaction rate is dominated by hydrogen pressure in view of its scant solubility in benzene, while the order with respect to the liquid reactant, benzene, will be zero. Under the gas-phase condition, the reaction-rate dependence will be different. For the present system, the reaction order for benzene will be greater than zero in the gas phase, since hydrogen is in large excess

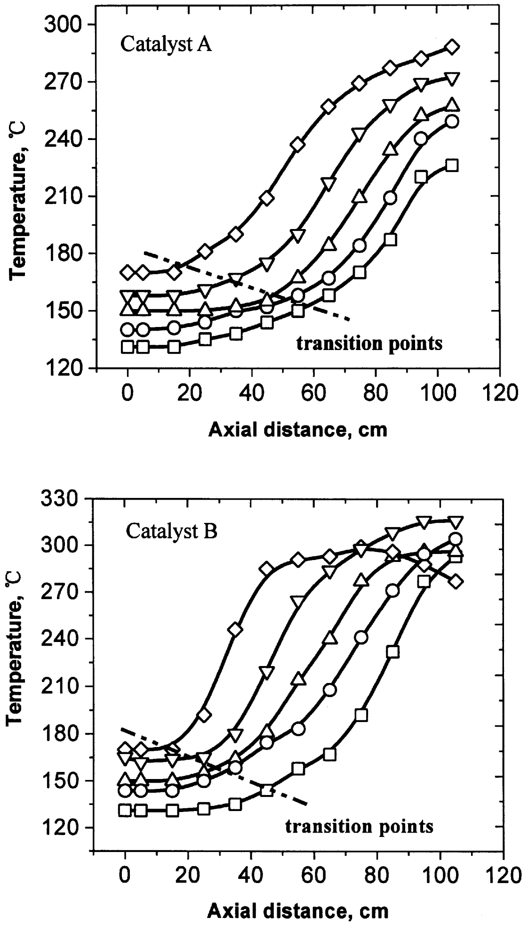

Figure 3. Influence of inlet temperature on liquid vanishing process.

$P_{sum} = 1.0$ MPa; $C_B^0 = 16.6\%$; $u_l = 1.46\times10^{-3}$ m/s; $u_g = 0.126$ m/s; $T_v = 117$°C. T_{in}, T_w: □—130°C; ○—140°C: △—150°C; ▽—160°C; ◇—170°C. Conversion: □, ○, △, ▽, ◇—100%.

for obtaining high conversion of benzene. Therefore, if the reaction rate is found to be independent of the benzene concentration at the inlet, the reaction can be considered to be in the liquid region.

Although a direct measurement of the reaction rate is not available, temperature measurements can be used instead, since the reactor is operated almost adiabatically. In Figure 4 it is observed that the reactor temperatures under different benzene concentrations fall into the same profile in the first 30 cm, which is considered to be the liquid region. Similar temperature profiles are also observed for Catalyst B, while the only difference is that the length of the liquid region is reduced from 30 cm to 10 cm, which is in agreement with the difference in the activity of the two catalysts. Further downstream, the variation in temperature with inlet feed concentration indicates that the reaction rate is a function of benzene concentration. This implies that in this region the reaction occurs in the gas phase, and therefore evaporation has occurred.

The preceding experimental results indicate that the liquid phase can exist above the vanishing temperature, T_v, which is in conflict with the theoretical speculation. This discrepancy can be rationalized by considering $T > T_v$ as a necessary condition, rather than a sufficient one for dryout. The existence of liquid phase over the vanishing point, T_v, can be explained by considering the boiling point of the mixture of benzene and cyclohexane. At 1.0 MPa, the boiling point is 180°C, which is 63°C and 65°C above the two T_v values shown in Figures 4 and 5. Since the boiling point of the liquid is greater than T_v, the liquid can be thermodynamically stable despite the inlet temperature being above T_v. Thus, an improved vapor–liquid equilibrium model is required for more accurate predictions of T_v in comparison to Raoult's law.

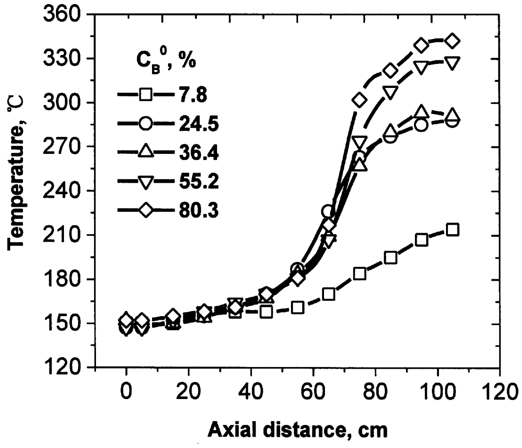

Figure 4. Identification of liquid region from concentration experiments for Catalyst A (the less active catalyst).

$P_{sum} = 1.0$ MPa, $u_l = 1.46\times10^{-3}$ m/s; $u_g = 0.126$ m/s; $T_{in} = T_w = 150$°C; $T_v = 117$°C. H_2/C_6H_6: □ — 33.6; ○—10.7; △ —7.2; ▽ —4.8; ◇—3.3. Conversion: □, ○—100%; △—53.3%; ▽—44.5%; ◇—37.0%.

Experimental dependence of liquid-region length

Verification of the existence of the liquid phase provides a qualitative description of the present subject; however, this

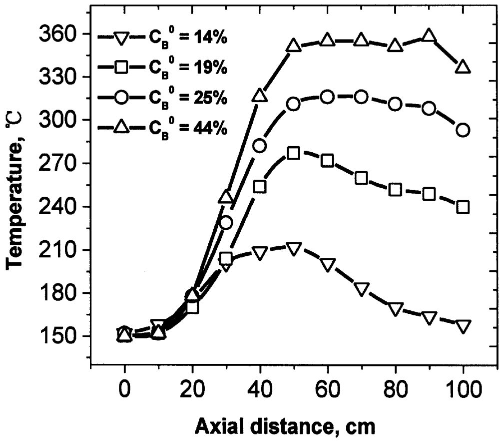

Figure 5. Identification of liquid region from concentration experiments for Catalyst B (the more active catalyst).

$P_{sum} = 1.0$ MPa, $u_l = 1.36\times{}^{-3}$m/s; $u_g = 0.126$ m/s; $T_{in} = T_w = 150$°C; $T_v = 115$°C. H_2/C_6H_6: ▽—19.9; □—11.2; ○—8.55; △—6.3. Conversion: ▽, □, ○, △—100%.

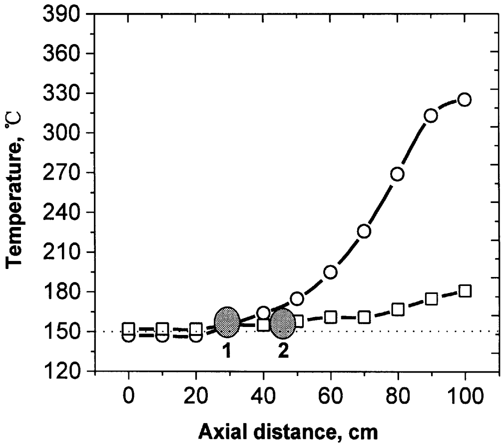

Figure 6. Effect of liquid flow rate on phase transition for Catalyst B.

$P_{\text{sum}} = 1.0$ MPa; $C_B^0 = 31.5\%$; $u_g = 0.126$ m/s; $T_{in} = T_w = 150°C$. u_l: ○—3.58×10^{-3} m/s; □—5.24×10^{-3} m/s. T_v: ○—142°C; □—152°C. Conversion: ○—41%; □—14%. Phase transition point: 1— 30 cm; 2— 45 cm.

information is insufficient for a complete understanding of the phase-transition process. For this purpose, various factors, including catalyst activity, liquid flow rate, gas flow rate, and the operation pressure, need to be studied.

The influence of catalyst activity can be observed in Figures 4 and 5, where it is found that the liquid-region length is inversely proportional to the catalyst activity, and thereby the reaction rate. Experiments under different liquid flow rates are shown in Figure 6. The liquid-region length is found to be approximately proportional to the liquid flow rate, which implies that the heat required for liquid vaporization under the adiabatic condition is only supplied by the reaction heat.

Figure 7 shows the experimental results for operation at different gas flow rates. The gas flow rate can greatly reduce the liquid vanishing temperature, and therefore increase the liquid evaporating rate. However, an obvious decrease in temperature profile was obtained in the liquid region under a gas flow rate of 0.126 m/s. This can be explained by the much faster vaporization of the liquid than in the other cases, due to the much lower vanishing temperature. In spite of these details, the gas flow rate has almost no effect on the length of the liquid region.

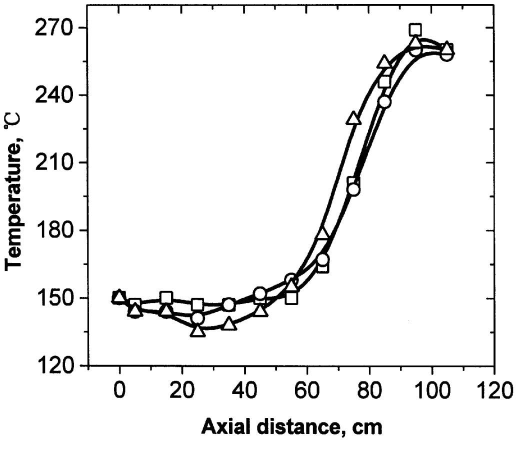

Figure 7. Effect of gas flow rate on phase transition for Catalyst A.

$C_B^0 = 21.2\%$; $P_{\text{sum}} = 1.0$ MPa; $L = 0.88 \times 10^{-3}$ m/s; $T_{in} = T_w = 150°C$. u_g: □—0.064 m/s; ○—0.088 m/s; △—0.126 m/s. T_v: □—123°C; ○—113°C; △—102°C. Conversion: □, ○, △—100%.

The pressure effect on phase transition is somewhat complex, as is shown in Figure 8. In this figure, two kinds of liquid inlet temperature, T_{in}, are employed, that are above or below T_v. When T_{in} is higher than T_v, the liquid-region lengths are the same, while when T_{in} is lower than T_v, the liquid-region lengths show some difference. This is because, in this case, the inlet liquid temperature has not reached the phase-transition temperature, so that the heat of the reaction will be used first to increase the system temperature and then for the vaporization. Therefore, enlargements of the liquid region under 2.5 and 3.0 MPa are observed in comparison with the other low-pressure cases.

Estimating the length of the liquid region

The liquid-region length can be estimated from the heat balance between the reaction heat and the vaporization heat of the liquid fluid. Assume that the superficial liquid velocity is u_l, the reaction rate in the liquid phase is r, and the reaction heat and the vaporization heat are ΔH_r and ΔH_v, respectively. Then the liquid-region length, L, can be approximated as

$$L = u_l \cdot \frac{l}{r} \cdot \frac{\Delta H_v}{\Delta H_r}, \tag{18}$$

which assumes relative constant temperature and reaction rate in the liquid region. This is consistent with the experimental observations in Figures 3 to 8. It should be noted that Eq. 18 applies only to the situation where liquid temperature is above the vanishing temperature. The validity of this equation in the reaction rate, r, has been verified from experiments under different catalyst activities, which shows the liquid-region length to be inversely proportional to the catalyst activity. Experiments under different liquid flow rates have verified the linear relationship between L and u_l, as can be observed from Figure 6. It should be noted that the liquid vanishing temperature, T_v, is not involved in Eq. 18, since this variable is not related to heat balance, and this consideration has been confirmed from experiments under the different gas flow rates shown in Figure 7.

Conclusions

The liquid vanishing process as well as the dryout phenomena in a three-phase fixed-bed reactor have been investigated. The vanishing point is defined as the point where the liquid flow rate is zero from the thermodynamic condition without considering whether or not sufficient energy is available for evaporation of the liquid phase. In the experiments, it was found that a certain entry length is needed before the liquid flow rate becomes zero, even when the inlet temperature is above the vanishing temperature, since the reaction heat in the entry region produces the required heat for liquid vanishing.

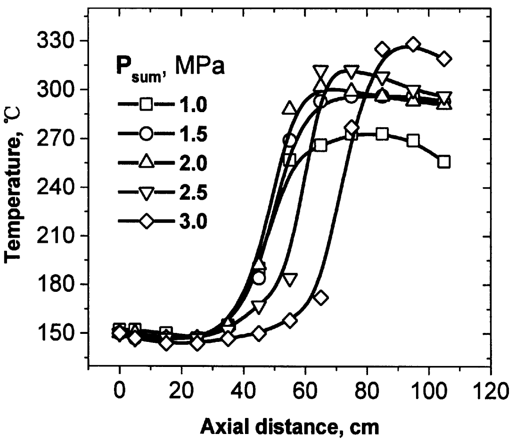

Figure 8. Effect of pressure on phase transition for Catalyst B.

$C_B^0 = 26.0\%$, $u_l = 1.16 \times 10^{-3}$ m/s; $u_g = 0.126$ m/s; $T_{in} = T_w = 150$°C. T_v: □—111°C; ○—128°C; △—140°C; ▽—152°C; ◇—162°C.

The liquid temperature can stay nearly constant in the entry section of the reactor before all the liquid has been vaporized. The length of the liquid region can be estimated from the heat balance between the reaction and vaporization, and is proportional to the liquid flow rate and the vaporization heat, but is inverse to the reaction rate and reaction heat.

Acknowledgments

The present work is supported by the Natural Science Foundation of China under Grant No. 20106005 and by SINOPEC through Contract No. 201085. Dr. Cheng is grateful to the Distinguished Visiting Scholar Program granted by the Chinese government in supporting his research in the University of Queensland, Australia.

Notation

C_B^0 = inlet benzene concentration in dilution by cyclohexane, vol %
F = mass flow rate, mol/s
F_l = mass flow rate in liquid phase, mol/s
ΔH_r = reaction heat, kJ/mol
ΔH_v = vaporization heat of liquid, kJ/mol
K = equilibrium constant in Raoult's law
L = length of the liquid region, m
M, N = molar flow rate ratio of gas to the liquid
P_{sum} = total pressure of all components, MPa
$P^0(T)$ = saturated vapor pressure of the liquid at temperature T, MPa
r = reaction rate, mol/kgcat·s
T = temperature, °C
T_{in} = inlet temperature of the reactant mixture, °C
T_v = vanishing temperature of the liquid, °C
T_w = reactor wall temperature, °C
u_g = gas-phase flow rate, m/s
u_l = liquid-phase flow rate, m/s
x = molar fraction in liquid phase
y = molar fraction in vapor phase

Greek letters

α = conversion of the reactant

Superscripts and Subscripts

0 = initial state
A = liquid reactant
B = gas reactant
C = liquid product
l = liquid phase
v = vapor phase

Literature Cited

Bhatia, S. K., "Steady State Multiplicity and Partial Internal Wetting of Catalyst Particles," *AIChE J.*, **34**, 969 (1988).

Bhatia, S. K., "Partial Internal Wetting of Catalyst Particles with a Distribution of Pore Size," *AIChE J.*, **35**, 1337 (1989).

Castellari, A. T., J. O. Cechini, L. J. Gabarain, and P. M. Haure, "Gas-Phase Reaction in a Trickle-Bed Reactor Operated at Low Liquid Flow Rates," *AIChE J.*, **43**, 1813 (1997).

Cheng, Z. M., A. M. Anter, and W. K. Yuan, "Intensification of Phase Transition on Multiphase Reactions," *AIChE J.*, **47**, 1185 (2001a).

Cheng, Z. M., A. M. Anter, G. M. Khalifa, J. S. Hu, Y. C. Dai, and W. K. Yuan, "An Innovative Reaction Heat Offset Operation for a Multiphase Fixed Bed Reactor Dealing with Volatile Compounds," *Chem. Eng. Sci.*, **56**, 6025 (2001b).

Cheng, Z. M., and W. K. Yuan, "Influence of Hydrodynamic Parameters on Performance of a Multiphase Fixed-Bed Reactor under Phase Transition." *Chem. Eng. Sci.*, **57**, 3407 (2002).

Hanika, J., K. Sporka, V. Ruzicka, and J. Krausova, "Qualitive Observations of Heat and Mass Transfer Effects on the Behaviour of a Trickle Bed Reactor," *Chem. Eng. Commun.*, **2**, 19 (1975).

Hanika, J., K. Sporka, V. Ruzicka, and J. Hrstka, "Measurement of Axial Temperature Profiles in an Adiabatic Trickle Bed Reactor," *Chem. Eng. J.*, **12**, 193 (1976).

Hanika, J., K. Sporka, V. Ruzicka, and R. Pistek, "Dynamic Behavior of an Adiabatic Trickle Bed Reactor," *Chem. Eng. Sci.*, **32**, 525 (1977).

Hanika, J., B. N. Lukjanov, V. A. Kirillov, and V. Stanek, "Hydrogenation of 1,5-Cyclooctadiene in a Trickle Bed Reactor Accompanied by Phase Transition," *Chem. Eng. Commun.*, **40**, 183 (1986).

Hanika, J., "Safe Operation and Control of Trickle-Bed Reactor," *Chem. Eng. Sci.*, **54**, 4653 (1999).

Hessari, F. A., and S. K. Bhatia, "Reaction Rate Hysteresis in a Single Partially Internally Wetted Catalyst Pellet: Experiment and Modelling," *Chem. Eng. Sci.*, **51**, 1241 (1996).

Hu, R., and T. C. Ho, "Steady State Multiplicity in an Incompletely Wetted Catalyst Particle," *Chem. Eng. Sci.*, **23**, 1239 (1987).

Jaguste, D. N., and S. K. Bhatia, "Partial Internal Wetting of Catalyst Particles: Hysteresis Effects," *AIChE J.*, **37**, 650 (1991).

Khadilkar, M. R., P. L. Mills, and M. P. Dudukovic, "Trickle-Bed Reactor Models for Systems with a Volatile Liquid Phase," *Chem. Eng. Sci.*, **54**, 2421 (1999).

Kheshgi, H. S., S. C. Reyes, R. Hu, and T. C. Ho, "Phase Transition and Steady-State Multiplicity in a Trickle-Bed Reactor," *Chem. Eng. Sci.*, **47**, 1771 (1992).

Kim, D. H., and Y. G. Kim, "An Experimental Study of Multiple Steady States in a Porous Catalyst due to Phase Transition," *J. Chem. Eng. Jpn.*, **14**, 311 (1981a).

Kim, D. H., and Y. G. Kim, "Simulation of Multiple Steady States in a Porous Catalyst due to Phase Transition," *J. Chem. Eng. Jpn.*, **14**, 318 (1981b).

LaVopa, V., and C. N. Satterfield, "Some Effects of Vapor-Liquid Equilibria on Performance of a Trickle-Bed Reactor," *Chem. Eng. Sci.*, **43**, 2175 (1988).

Ramakrishna, V. N., J. A. Guin, A. R. Tarrer, and C. W. Curtis, "Effect of Phase Behavior on Hydrotreater Performance: Simulation and Experimental Verification," *Ind. Eng. Chem. Process Des. Dev.*, **24**, 598 (1985).

Reid, R. C., J. M. Prausnitz, and T. K. Sherwood, *The Properties of Gases and Liquids,* 4th ed., McGraw-Hill, New York (1987).

Ruzicka, J., and J. Hanika, "Partial Wetting and Forced Reaction Mixture Transition in a Model Trickle-Bed Reactor," *Catal. Today*, **20**, 467 (1994).

Sedriks, W., and C. N. Kenney, "Partial Wetting in Trickle Bed Reactors—The Reduction of Crotonaldehyde over a Palladium Catalyst," *Chem. Eng. Sci.*, **28**, 559 (1973).

Singh, C. P. P., and N. L. Carr, "Process Simulation of an SRC—II Plant," *Ind. Eng. Chem. Process Des. Dev.*, **22**, 104 (1983).

Smith, C. M., and C. N. Satterfield, "Some Effects of Vapor–Liquid Flow Ratio on Performance of a Trickle-Bed Reactor," *Chem. Eng. Sci.*, **41**, 839 (1986).

Watson, P. C., and M. P. Harold, "Dynamic Effects of Vaporization with Exothermic Reaction in a Porous Catalyst Pellet," *AIChE J.*, **39**, 989 (1993).

Watson, P. C., and M. P. Harold, "Rate Enhancement and Multiplicity in a Partially Wetted and Filled Pellet: Experimental Study," *AIChE J.*, **40**, 97 (1994).

Manuscript received Nov. 16, 2000, and revision received July 11, 2002.